ORIGINAL ARTICLE

The proteasome inhibitor bortezomib targets cell cycle and apoptosis and acts synergistically in a sequence-dependent way with chemotherapeutic agents in mantle cell lymphoma

Grit Hutter · Malte Rieken · Alessandro Pastore · Oliver Weigert · Yvonne Zimmermann · Marc Weinkauf · Wolfgang Hiddemann · **Martin Dreyling**

Received: 17 August 2011 / Accepted: 19 November 2011 / Published online: 11 January 2012 © Springer-Verlag 2012

Abstract Single-agent bortezomib, a potent, selective, and reversible inhibitor of the 26S proteasome, has demonstrated clinical efficacy in relapsed and refractory mantle cell lymphoma (MCL). Objective response is achieved in up to 45% of the MCL patients; however, complete remission rates are low and duration of response proved to be relatively short. These limitations may be overcome by combining proteasome inhibition with conventional chemotherapy. Rational combination treatment and schedules require profound knowledge of underlying molecular mechanisms. Here we show that single-agent bortezomib treatment of MCL cell lines leads to G2/M arrest and induction of apoptosis accompanied by downregulation of EIF4E and CCND1 mRNA but upregulation of p15(INK4B) and p21 mRNA. We further present synergistic efficacy of bortezomib combined with cytarabine in MCL cell lines. Interestingly this sequence-dependent synergistic effect was seen almost exclusively in combination with AraC, indicating that pretreatment with cytarabine, followed by proteasome inhibition, may be the preferred approach.

A. Pastore · O. Weigert · W. Hiddemann · M. Dreyling Munich, Germany

G. Hutter () · A. Pastore · O. Weigert · Y. Zimmermann · M. Weinkauf · M. Dreyling Helmholtz Centre Munich, Marchioninistr. 25, 81377 Muenchen, Germany e-mail: hutter@helmholtz-muenchen.de

M. Rieken Urologische Klinik, Universitätsspital Basel, Basel, Switzerland

Department of Medicine III, University Hospital Grosshadern,

Keywords MCL · Bortezomib · AraC · Apoptosis · Cell cycle arrest

Introduction

The ubiquitin-proteasome pathway is essential for maintaining intracellular protein homeostasis and represents a valid target for the treatment of malignant disease [1, 2]. At the center of this highly coordinated degradation pathway is the 26S proteasome, an abundant ATP-dependent multicatalytic protease. Various oncogenes and regulatory proteins for cell cycle progression and apoptosis are processed by this pathway [3, 4]. Bortezomib is a potent, selective, and reversible inhibitor of the catalytic 20S subunit of the proteasome, specifically the chymotryptic threonine protease activity as the rate-limiting enzymatic step. Besides its proven efficacy in relapsed multiple myeloma [5, 6], single-agent bortezomib demonstrated clinical activity in several other hematologic malignancies [7, 19] with especially encouraging results being observed in patients with relapsed or refractory mantle cell lymphoma (MCL) [8–13]. Objective response is achieved in up to 45% of the MCL patients; however, complete remission rates are low and duration of response proved to be relatively short. These limitations may be overcome by combining proteasome inhibition with conventional chemotherapy [14–16]. The clinical feasibility of such an approach has been demonstrated for liposomal doxorubicin in patients with various advanced hematologic malignancies [17]. Considering the abundant presence and necessity of proteasome activity in every eukaryotic cell,



surprisingly little toxicity is observed using bortezomib in clinical practice with mild thrombocytopenia, peripheral neuropathy, and low-grade diarrhea being most common [18, 19], rendering this agent highly attractive for combination treatment. Synergism of bortezomib has been described with numerous other targeted approaches including the small-molecule pan-BCL2 inhibitor GX15-070 [20], the farnesyltranseferase inhibitor R115777 [21], the mTOR inhibitor RAD001 [22], the histone deacetylase inhibitor SAHA [23], the BH3-only mimetic ABT-737 [24], the HDM-2/p53 ligase inhibitor MI-63 [25], and the small-molecule murine double minute 2 antagonist Nutlin-3 [26].

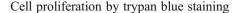
The underlying reasons for the particular susceptibility of proliferating and especially transformed cells remain incompletely understood. In response to disruption of protein turnover by a reversible proteasome inhibitor like bortezomib, normal cells seem to have the ability to activate checkpoint mechanisms to arrest cell division and resume proliferation after proteasome activity is restored, whereas most malignant cells have dysfunctional checkpoint mechanisms [27].

Rational combination treatment and schedules require profound knowledge of underlying molecular mechanisms; however, astonishingly little is known about down-stream events caused by proteasome inhibition in mantle cell lymphoma.

Materials and methods

Cells and reagents

Established MCL cell lines consisted of Granta-519, HBL-2, Jeko-1, NCEB-1, and Rec-1. The human T-cell leukemia cell line Jurkat, the human follicular B-cell lymphoma cell line Karpas 422 and the MEC1, MEC2 CLL cell lines were used as hematological control cell lines. All cell lines were purchased from the German Collection of Microorganisms and Cell Cultures (DSMZ, Braunschweig, Germany) and cultured in RPMI 1640 culture medium (PAN, Aidenbach, Germany) and MDM (MEC1, MEC2) at 37°C in a humified atmosphere containing 5% carbon dioxide. Culture medium was supplemented with 20% heat-inactivated fetal calf serum (FCS; Granta-519, Jeko-1, NCEB-1, and REC-1) and 10% FCS (HBL-2, MEC1, MEC2, Jurkat, and Karpas 422), respectively. Bortezomib was provided by Janssen-Cilag (Velcade®, Neuss, Germany), cytarabine was purchased from Cell Pharm (Ara-Cell®, Hannover, Germany), fludarabine from Medac GmbH (Wedel), gemcitabine from Eli Lilly (Wien, Austria), and mitoxantrone from Hexal AG (Holzkirchen).



Cells were seeded at a density of 5×10^5 /ml in the absence or presence of bortezomib (0–50 nM). Cells were counted using the ViCell Cell viability analyzer at 24, 48, and 72 h.

Apoptosis detection by annexin V staining

For apoptosis assay, cells were analyzed by flow cytometry 0, 12, and 24 h after bortezomib exposure. Cells were washed and stained with Annexin V-PE and 7-AAD in accordance with the manufacturer's protocol (BD Biosciences, Heidelberg, Germany). Apoptosis was assessed by flow cytometry (BD FACS Calibur System, BD Biosciences, Palo Alto, CA, USA) and WinMDI 2.8 Software (Joseph Trotter). Apoptosis rate was calculated as follows:

$$\left(1 - \frac{\text{"fraction variable treated cells"}}{\text{"fraction variable untreated cells"}} \times 100\%\right)$$
.

Cell cycle analysis

 2×10^5 cells per tube were incubated with bortezomib (25nM) and cell cycle analysis was performed at 0, 4, 8, and 12 h in independent triplicates. Cells were washed, resuspended in 200 µl of lysis buffer (0.1% sodium citrate, 0.1% Triton X-100 (Sigma-Aldrich Chemie GmbH, Taufkirchen), 20 µg/ml propidium iodide (Sigma-Aldrich Chemie GmbH (Taufkirchen), and 100 µg/ml ribonuclease A (Merck KG, Darmstadt), and incubated on ice in the dark for 5 min. Flow cytometry was performed subsequently using BD FACS Calibur (BD Biosciences, Palo Alto, CA, USA). The percentage of cells in G_0/G_1 , S, and G_2/M phase was calculated using ModFit LT (Verity Software House, Inc., Topsham, MA, USA).

Cell viability assay and determination of Chou and Talalay's combination index

Cell viability correlates with the activity to metabolize the tetrazolium salt WST-1 to a water-soluble formazan dye, which is measured spectrophotometrically (Roche Applied Science, Mannheim, Germany). Cells were seeded at a density of $1\times10^6/\text{ml}$ in a 96-well microplate in triplicates (100.000 cells/well) and the assay was performed according to the manufacturer's protocol (Roche Applied Science, Mannheim, Germany). The following agents and concentrations were used: bortezomib (0–100 nM), cytarabine (0–25 µg/ml), fludarabine (0–10 µg/ml), gemcitabine (0–10 µg/ml), and mitoxantrone (0–5 µg/ml). Agents were diluted serially at a 1:1 ratio. After the incubation period (12 or 24 h), the WST-1 reagent was added and analyzed by an



ELISA reader (Optimax pro, Molecular Devices, Sunnyvale, CA) after another 4 h.

To determine synergistic, additive, or antagonistic effects of the drug combinations, the CalcuSyn software (Biosoft, Cambridge, UK) was used, which is based on the combination method of Chou and Talalay [28, 29]. This software was applied to calculate the combination index (CI) by taking into account the IC_{50} of each drug and the shape of the dose–effect curve.

The so determined index (CI) allows the identification of antagonistic ($\text{CI}_{50} \! > \! 1.3$), additive ($\text{CI}_{50} \! = \! 1 \pm \! 0.3$) or synergistic ($\text{CI}_{50} \! < \! 0.7$) efficacy of combination treatment by considering cell viability curves determined after 12 and 24 h of treatment with the chemotherapeutic agent alone, bortezomib alone, or in combination (synchronous and sequential incubation) of both, respectively. Due to experimental design however, a small number of estimations with exceedingly high standard deviations (>50% of CI_{50}) were unavoidable and marked accordingly.

Real-time RT-PCR

Total RNA extraction was performed with RNeasy Kit (Qiagen, Hilden, Germany) in accordance with the manufacturer's protocol. RNA was retrotranscribed using GeneAmp® Gold RNA PCR Kit (Applied Biosystems, Darmstadt, Germany). Real-time polymerase chain reaction (RT-PCRs) was performed using Taqmanassays (Applied biosystems) for CCND1, EIF4E, p15(INK4B), p21, AKT1, and RT Primer sets from Qiagen (Qiagen, Hilden) for GSK3A, GSK3B, RPS6, BCL2, CDK2, CDK4, CDK7, CDK9, and 4EBP1 mRNA expression levels were quantified relatively and normalized against the TBP transcript abundance. RT-PCR experiment data were obtained from three independent experiments.

Statistical analysis

 CI_{50} value was calculated with Calcusyn® (Biosoft, Cambridge, UK).

Results

Inhibition of cell proliferation by single-agent bortezomib

Impact of single-agent bortezomib on cell proliferation of MCL and other hematologic cell lines was initially assessed by trypan blue staining. All tested cell lines demonstrated a time- and dose-dependent inhibition of cell proliferation (Fig. 1). With the exception of two control cell lines (Karpas 422, MEC2), the proliferation of all mantle cell lymphoma cell lines and two other control cell lines (Jurkat, MEC1)

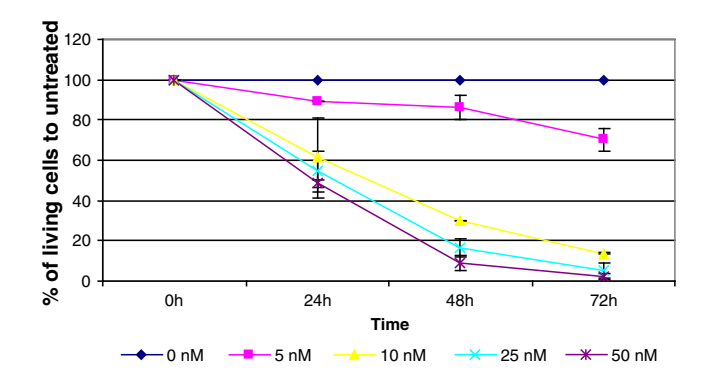
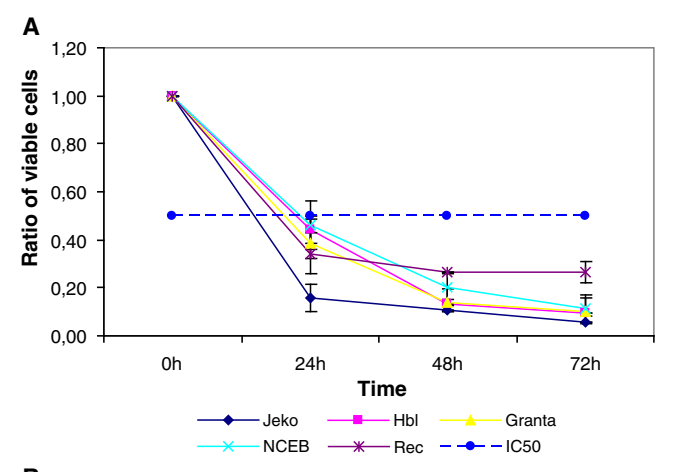


Fig. 1 Time- and dose-dependent inhibition of cell proliferation by single-agent bortezomib. Cells were counted by the ViCell Cell viability analyzer after incubation with single-agent bortezomib [0–25 nM] at various time points. Numbers of cells are depicted in percentage of untreated control cells (Representative data of Granta-519)

decreased to less than 50% after bortezomib exposure at a clinically representative concentration of 25 nM (Fig. 2a, b). Interestingly the two cell lines MEC1 and MEC2



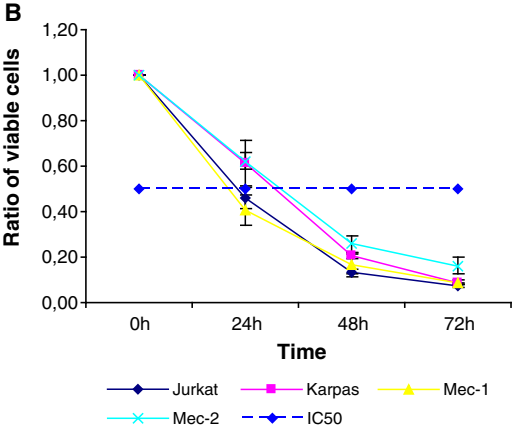


Fig. 2 Time-dependent inhibition of cell proliferation by single-agent bortezomib. Cells were counted by the ViCell Cell viability analyzer after incubation with single-agent bortezomib [25 nM] at various time points. Numbers of cells are depicted in relation to untreated control cells. **a** Mantle cell lymphoma cell lines. **b** Control cell lines (*MEC1*, *MEC2* B-CLL, *Karpas 422* B-cell NHL, *Jurkat* human T-cell leukemia)



established from the same patient with a B-CLL in prolymphocytoid transformation, one prior to therapy (MEC1) and the other after therapy (MEC2), showed different sensitivity to bortezomib (Fig. 2b), indicating an inducible mechanism of bortezomib resistance.

These results were confirmed by WST-1 assay. Cells were incubated with single-agent bortezomib (0–100 nM) and analyzed after an incubation period of 24 h. The IC₅₀ values are listed in Table 1. Except for NCEB-1, the IC₅₀ values were within a clinically achievable dose range. Jeko-1 was demonstrated to be most sensitive, whereas Granta-519, HBL-2, and Rec-1 showed only intermediate sensitivity after 24 h of exposure to bortezomib. Of note, the hematological control cell lines Jurkat and Karpas 422, demonstrated moderate sensitivity to single-agent bortezomib.

Analysis of apoptosis after bortezomib exposure

To determine the apoptosis-inducing potential of bortezomib, cells were exposed to single-agent bortezomib at a dose of 25 nM and analyzed by flow cytometry at 0, 12, and 24 h. Time-dependent induction of apoptosis could be detected in all cell lines after 12 and 24 h; however, results demonstrated a wide range of susceptibility (Fig. 3). Consistent with the results of the WST-1 assay, Jeko-1 was most sensitive to induction of apoptosis whereas Granta-519, HBL-2, and Rec-1 showed intermediate sensitivity. Again, NCEB-1 demonstrated to be least susceptible to bortezomib treatment. In the control cell lines (Karpas 422, Jurkat), only moderate induction of apoptosis could be shown.

Cell cycle analysis after bortezomib exposure

To detect cell cycle alterations following proteasome inhibition, cells were analyzed after 0, 4, 8, and 12 h of bortezomib exposure. Changes in the cell cycle profile could be seen already after 4 or 8 h of treatment. A "sub-Go/G1" peak, corresponding to apoptotic cells, was detected in all cell lines depending on previously observed susceptibility to bortezomib treatment (Fig. 4). The most prominent changes could be seen in the Hbl-2 cell line with the percentage of

Table 1 Impact of bortezomib and conventional chemotherapeutic agents on cell proliferation

IC₅₀ values [μg/ml] by WST-1 assay after incubation with

IC₅₀ values [μg/ml] by WST-1 assay after incubation with bortezomib, cytarabine, fludarabine, gemcitabine, and mitoxantrone *NR* not reached

	Bortezomib	Cytarabine	Fludarabine	Gemcitabine	Mitoxantrone
Granta-519	22.093±6.42	17.49±5.48	0.9±0.2	0.61±0.29	0.23±0.1
HBL-2	25.001 ± 4.99	3.81 ± 1.69	0.51 ± 0.14	0.11 ± 0.1	0.42 ± 0.33
Jeko-1	17.16 ± 4.23	2.3 ± 1.49	0.73 ± 0.69	0.17 ± 0.07	0.59 ± 0.39
NCEB-1	39.19 ± 12.18	NR	0.13 ± 0.076	1.63 ± 0.205	0.68 ± 0.23
Rec-1	28.19 ± 0.36	NR	NR	NR	3.92 ± 0.354
Jurkat	29.08 ± 9.56	3.85 ± 2.46	0.31 ± 0.18	0.08 ± 0.059	0.12 ± 0.051
Karpas 422	27.219 ± 5.47	3.7 ± 0.68	0.53 ± 0.17	0.11 ± 0.12	0.75 ± 0.06

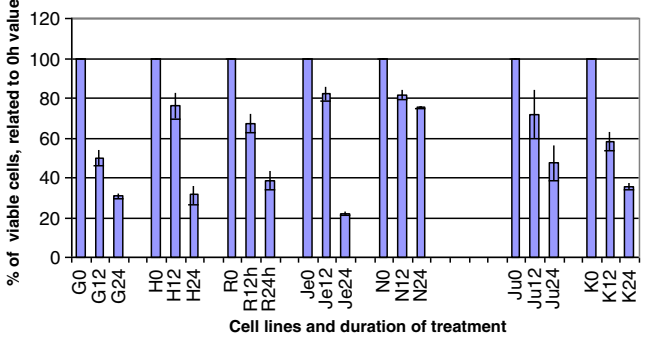


Fig. 3 Induction of apoptosis by single-agent bortezomib (25 nM). Cells were stained with Annexin V-PE and 7-AAD and analyzed by flow cytometry after 0, 12, and 24 h of incubation. *G* Granta-519, *H* Hbl-2, *R* Rec-1, *Je* Jeko-1, *N* NCEB-1, *Ju* Jurkat, *K* Karpas 422

cells in the G2/M phase increasing from 20.5% to 44.5% and those in G0/G1 phase decreasing from 48% to 27%. In Granta-519, changes towards a G2/M cell cycle arrest were also observed. Only little impact on cell cycle was observed in the less sensitive cell lines, NCEB-1 and Rec-1. Thus, the grade of cell cycle alterations directly correlated to proliferation inhibition. In the control cell lines (Karpas 422, Jurkat) moderate G2/M cell cycle arrest was also detected in a sensitivity-dependent manner.

Bortezomib induced downregulation of CCND1 but upregulation of BCL2 and CDK inhibitor p21 RNA

To further analyze the impact of bortezomib on central regulator genes of cell cycle and apopotosis, real-time RT-PCR analysis of MCL cell lines and control cell lines cultured in the presence or absence of bortezomib (25 nM at 24 h) was performed. After a 24-h exposure to bortezomib, CCND1 mRNA was downregulated in all of the MCL cell lines (Fig. 5a). This downregulation was accompanied by a decrease of EIF4E RNA expression (Fig. 5b). Upregulation of p21 RNA was detected in four out of five MCL and in both control cell lines while p15 (INK4B) was upregulated in two out of the five MCL cell lines and in one of the control cell lines (Fig. 5c). In contrast to the other MCL cell lines, Hbl-2 did not express GSK3A RNA but therefore



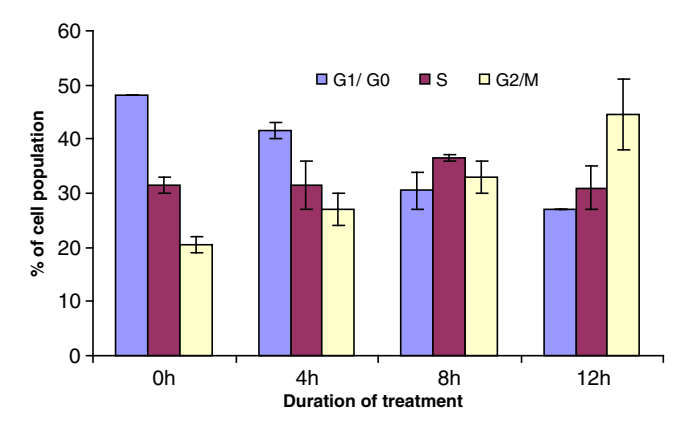
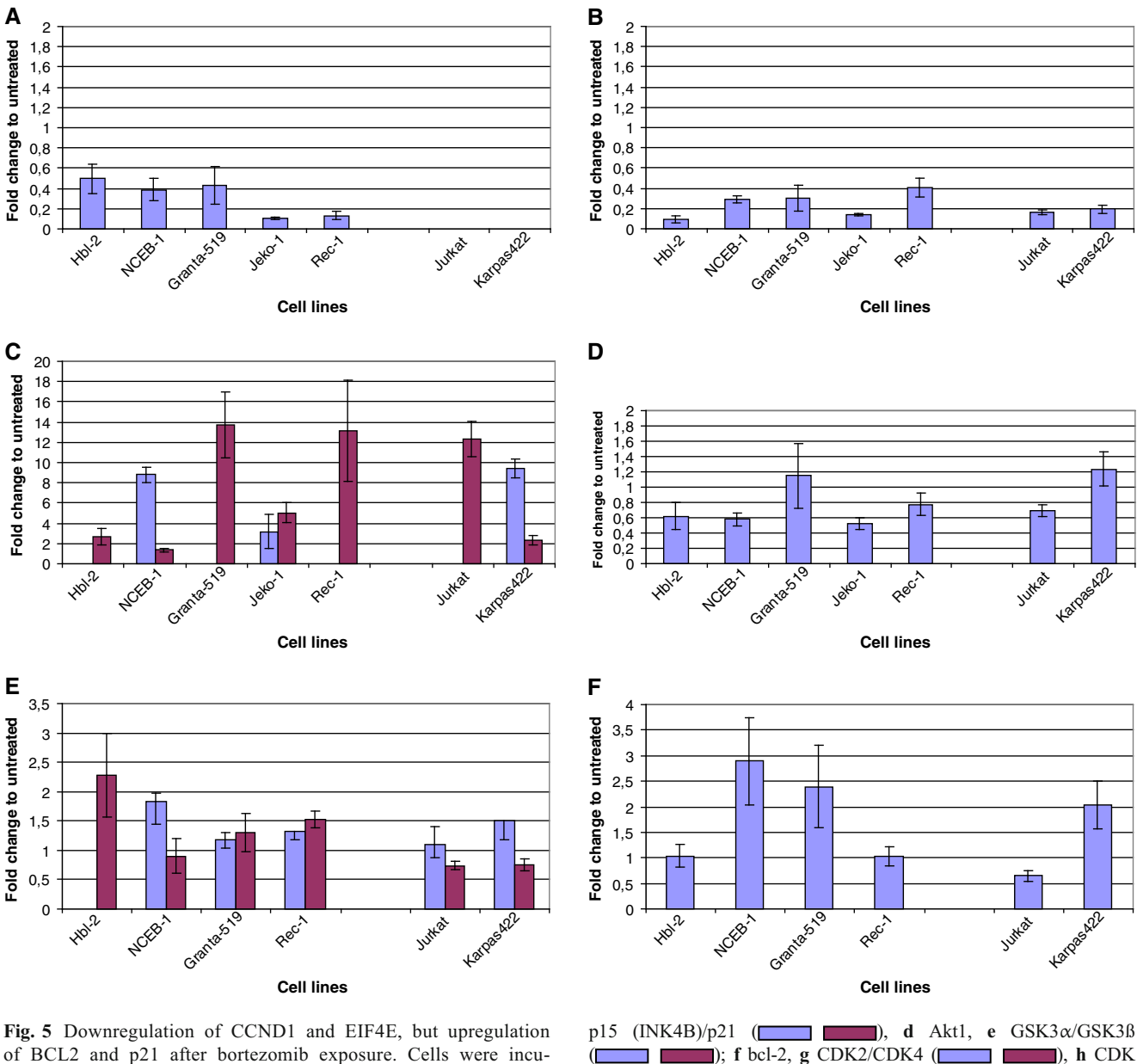


Fig. 4 Cell cycle profile after bortezomib treatment (cell line Hbl-2)

revealed an upregulation of GSK3ß RNA while in all other MCL cell lines the GSK3ß and GSK3A mRNA expression remained nearly unchanged (Fig. 5e). Interestingly GSK3BRNA was downregulated in the control cell lines (Fig. 5e). AKT1 RNA was downregulated in three out of five MCL cell lines and in one of the control cell lines (Fig. 5d). Interestingly BCL2 RNA was upregulated in two out of four MCL cell lines and one of the control cell lines after bortezomib treatment (Fig. 5f).

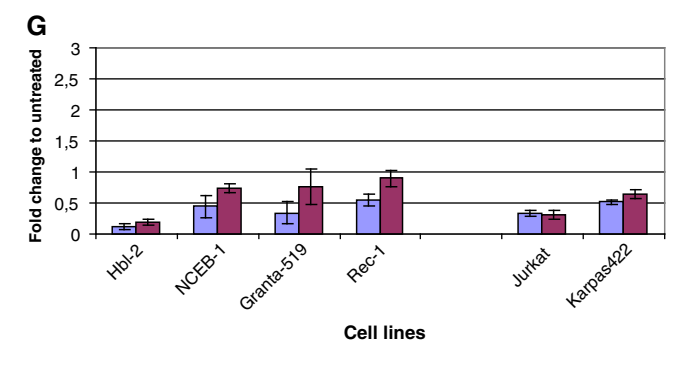
Bortezomib exposure did impair the RNA expression of CDK2 and CDK4 stronger than that of CDK7and CDK9 (Fig. 5g, h). 4EBP1 RNA was downregulated in all cell lines except one (Granta-519; Fig. 5i).

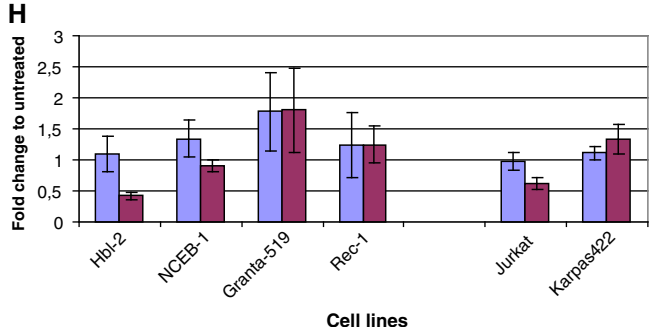


of BCL2 and p21 after bortezomib exposure. Cells were incubated with 25 nM bortezomib and analyzed by real-time PCR for their RNA expression profile after 24 h. a CyclinD1. b EIF4A. c









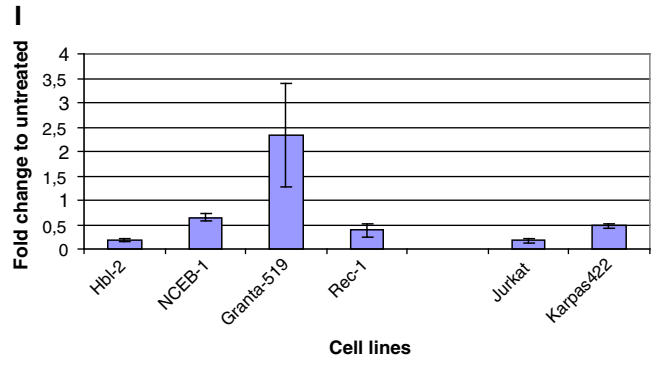


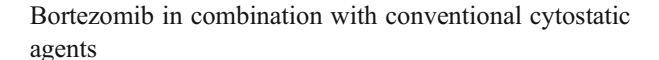
Fig. 5 (continued)

Effect of conventional cytostatic agents on MCL cells

Cells were exposed to clinically established cytostatic agents, encompassing the cell phase (S) specific antimetabolites cytarabine (0–25 μ g/ml), fludarabine (0–10 μ g/ml), and gemcitabine (0–10 μ g/ml) as well as the anthracyclin analogue mitoxantrone (0–5 μ g/ml), which is known to exhibit cytotoxicity throughout the cell cycle. IC₅₀ values at 24 h of incubation were determined using WST-1 assay. Results are listed in Table 1.

Both the MCL cell line Rec-1 and the non-MCL cell line Karpas 422 were relatively resistant to all antimetabolites, with the IC_{50} not reached within the applied dose range. Similarly, in NCEB-1, an IC_{50} could not be reached for cytarabine and required IC_{50} doses of gemcitabine and mitoxantrone were higher than in the remainder cell lines. In contrast, fludarabine was surprisingly effective in NCEB-1.

Cytotoxicity of cytarabine varied significantly between cell lines with high proliferation inhibition in Jeko-1, HBL-2, and Jurkat, but intermediate in Granta-519. Fludarabine at concentrations of <1 $\mu g/ml$ induced cytotoxicity in all cell lines except Rec-1 and Karpas 422. Gemcitabine was effective at very low doses in all cell lines again except again Rec-1 and Karpas 422. While Granta-519, HBL-2, and Jeko-1 were particularly sensitive to even very low doses of mitoxantrone, Rec-1, NCEB-1, and Karpas 422 tolerated higher concentrations.



To determine the potential of proteasome inhibition to induce synergistic cytotoxicity if combined with conventional chemotherapeutic agents, cells were exposed to bortezomib plus either cytarabine, fludarabine, gemcitabine, or mitoxantrone, respectively. Efficacy of combination treatment was estimated using the CI at IC_{50} according to Chou and Talalay's equation. Sequential exposures (addition of second agent after 12 h) were examined. The results of sequential experiments are listed in Tables 2, 3, 4, and 5.

Despite the complexity of the data, two distinct patterns of cytotoxicity to combination treatment were identified. All MCL cell lines but NCEB demonstrated significant synergistic cytotoxicity if sequentially exposed to cytarabine followed by addition of bortezomib (Table 2). Exposure to the same agents vice versa yielded antagonism in all MCL cell lines but Granta-519 and NCEB-1.

On the other hand, all MCL cell lines but NCEB-1 demonstrated significant antagonism if sequentially exposed to mitoxantrone followed by bortezomib thereafter (Table 3).

For the other chemotherapy combinations with either fludarabine or gemcitabine, such differential interactions could not be determined (Tables 4 and 5).



Table 2 Combination of bortezomib and cytarabine

Cell line	BZ 24 h + ARA-C 12 h	BZ 12 h + ARA-C 24 h
Granta-519	0.55 (±0.21)	0.50 (±0.08)
HBL-2	2.83 (±0.57)	0.17 (±0.05)
Jeko-1	1.60 (±0.81)	0.23 (±0.05)
NCEB-1	1.52 (±0.23)	1.11 (±0.34)
Rec-1	2.08 (±0.51)	0.15 (±0.16)
Jurkat	0.62 (±0.23)	0.46 (±0.22)
Karpas 422	1.32 (±0.34)	0.62 (±0.04)

CI values at IC $_{50}$ for the combination of bortezomib (BZ, either 12 or 24 h) and cytararbine (ARA-C, either 12 or 24 h). CI $_{50} \le 0.7$ denotes synergistic (green), $0.7 < \text{CI}_{50} < 1.3$ denotes additive, and CI $_{50} \ge 1.3$ denotes antagonistic (red) cytotoxicity

Discussion

Our in vitro data confirm the significant antilymphoma activity of bortezomib not only in five well-established and characterized MCL cell lines, but also in the T-cell leukemia cell line Jurkat and the follicular B-cell lymphoma cell line Karpas 422. Cell proliferation assessed by trypan blue staining as well as cell viability assessed by WST-1 assay was significantly inhibited by single-agent bortezomib in a dose and time-dependent manner. In accordance with the description of distinct in vitro patterns of karyotypic variability of established MCL cell lines [30], susceptibility to bortezomib treatment varied remarkably. Considering the proliferation-inhibiting potential of bortezomib we identified Jeko-1 as highly sensitive, whereas Granta-519, HBL-2, and Rec-1 showed only intermediate sensitivity after 24 h of exposure to bortezomib. The fact that NCEB-1 demonstrated to be the least sensitive cell line may be explained by a previous observation, that this cell line represents a mouse hybrid cell line with several stable mouse chromosomes showing expression of both human and murine bcl-2 protein [30]. Analysis of apoptosis and cell cycle analysis revealed also different patterns of response to bortezomib treatment.

Table 3 Combination of bortezomib and mitoxantrone

Cell line	BZ 24 h + MITO 12 h	BZ 12 h + MITO 24 h
Granta-519	0.61 (±0.19)	1.21 (±0.49)
HBL-2	0.92 (±0.18)	1.57 (±0.53)
Jeko-1	0.69 (±0.25)	1.69 (±0.34)
NCEB-1	1.14 (±0.72)	1.76 (±0.68)
Rec-1	0.93 (±0.47)	1.84 (±0.72)
Jurkat	1.74 (±0.38)	1.18 (±0.15)
Karpas 422	0.54 (±0.29)	1.35 (±0.22)

CI values at IC₅₀ for the combination of bortezomib (BZ) and mitoxantrone (MITO). $\text{CI}_{50} \leq 0.7$ denotes synergistic (green), $0.7 < \text{CI}_{50} < 1.3$ denotes additive, and $\text{CI}_{50} \geq 1.3$ denotes antagonistic (red) cytotoxicity

Table 4 Combination of bortezomib and fludarabine

Cell line	BZ 24 h + FLU 12 h	BZ 12 h + FLU 24 h
Granta-519	1.05 (±0.23)	1.01 (±0.23)
HBL-2	1.55 (±0.28)	0.89 (±0.13)
Jeko-1	3.65 (±0.46)	0.41 (±0.09)
NCEB-1	1.23 (±0.27)	0.86 (±0.07)
Rec-1	2.55 (±0.53)	0.66 (±0.39)
Jurkat	1.00 (±0.20)	0.86 (±0.71)
Karpas 422	2.38 (±0.91)	1.97 (±0.56)

CI values at IC₅₀ for the combination of bortezomib (BZ, either 12 or 24 h) and fludarabine (FLU either 12 or 24 h). $CI_{50} \le 0.7$ denotes synergistic (green), $0.7 < CI_{50} < 1.3$ denotes additive, and $CI_{50} \ge 1.3$ denotes antagonistic (red) cytotoxicity

While arrest in G2/M phase and induction of apoptosis were determined as the mechanism of response in sensitive MCL cell lines, neither relevant cell cycle alteration nor induction of apoptosis was observed in NCEB-1.

To identify an early and common pattern of downstream events after bortezomib exposure, quantitative real-time RT-PCR was performed. Constitutive overexpression of CCND1 is the molecular hallmark of MCL [31-33] and consequently inhibition of CCND1 has been considered as a potential therapeutic strategy. After bortezomib exposure, we could demonstrate a significant downregulation of mRNA levels of CCND1 in the MCL cell lines accompanied by a downregulation of EIF4E. It is well-known that p15(INK4B) is an upstream inhibitor of CCND1 and that p21 interferes with the formation of the cyclin/CDK complexes hematopoetic cells [34, 35]. Thus upregulation of p15(INK4B) and p21 could be the reason of the reduced CCND1 mRNA expression as well as the observed downregulation of CDK2 and CDK4. Similar results, G2/M phase arrest and downregulation of cyclinD1, have been shown recently in hepatocellular carcinoma cells with the G2/M cell cycle arrest after bortezomib exposure

Table 5 Combination of bortezomib and gemcitabine

Cell line	BZ 24 h + GEM 12 h	BZ 12 h + GEM 24 h
Granta-519	0.85 (±0.30)	0.17 (±0.04)
HBL-2	1.55 (±1.4)	1.46 (±0.40)
Jeko-1	3.65 (±0.86)	1.55 (±0.27)
NCEB-1	0.30 (±0.03)	7.04 (±1.34)
Rec-1	0.53 (±0.41)	2.12 (±0.69)
Jurkat	0.25 (±0.06)	0.29 (±0.08)
Karpas 422	0.74 (±0.23)	1.53 (±0.26)

CI values at IC_{50} for the combination of bortezomib (BZ, either 12 or 24 h) and gemcitabine (GEM, either 12 or 24 h). $CI_{50} \le 0.7$ denotes synergistic (green), $0.7 < CI_{50} < 1.3$ denotes additive, and $CI_{50} \ge 1.3$ denotes antagonistic (red) cytotoxicity



inducing transcriptional downregulation of cyclin D1 and upregulation of p21(Waf1/Cip1) [39].

We also analyzed EIF4E mRNA as experimental models have revealed eIF4E as an important regulator of malignant transformation and tumor growth [34]. EIF4E mRNA was downregulated by bortezomib treatment, which might also result in the downregulation of CCND1 mRNA translation [36, 37]. However, another protein, the potent, antiapoptotic kinase AKT, which has also been shown to be translationally controlled by EIF4E [38], was downregulated in most of the cell lines. The downregulated Akt1 mRNA could also lead to the downregulation of cyclinD1 RNA as AKT has been described to mediate expression of CCND1 protein [40] and increase CCND1 protein expression [41].

Previously it has been described that activated AKT protein decreases activation of human GSK3ß in 293t cells [42]. Downregulation of Akt1 mRNA by bortezomib could therefore explain the low impact on the mRNA expression profiles of GSK3α and GSK3β observed in the present study. The exceptional enhancement of GSK3ß mRNA in Hbl-2 might be the result from the absence of $GSK3\alpha$. Interestingly in the present study, there was a close relationship between EIF4E, CCND1, p15INK4B, and p21 mRNA expression in all the cell lines. In cases with CCND1 mRNA downregulation, EIF4E mRNA expression also went down, whereas p15INK4B and p21 mRNA were upregulated. Thus both cyclinD1, and CDKs (CDK2, CDK4, CDK7, CDK9) were regulated suggesting a strong impact of bortezomib on the cyclinD1/cdk4-Rb pathway. Interestingly the mRNA expression of the 4EBP1, which binds to EIF4E and is blocking cap-dependent translation initiation and is thereby linking translation initiation with the phosphatidylinositol 3kinase/Akt/mTOR signaling pathway, was downregulated after bortezomib treatment in most of the cell lines. Therefore the common downregulation of Akt1, 4EBP1, EIF4E, and cyclinD1 RNA upon exposure to bortezomib suggests the involvement of the phosphatidylinositol 3-kinase/Akt/ mTOR signaling pathway by translation initiation.

Previous reports indicate that not all lymphoma cells are sensitive to bortezomib. However as our results indicate that bortezomib modulates survival and antiapoptotic pathways, treated cells may be sensitized to cytotoxic stimuli including conventional chemotherapy resulting in an overadditive synergy. Accordingly Ma et al. could demonstrate a markedly increase of sensitivity of chemoresistant myeloma cells (100,000–1,000,000-fold) when chemotherapy was combined with a noncytotoxic dose of bortezomib without affecting normal hematopoietic cells. Similar effects were observed using a dominant negative super-repressor for IkkBalpha [43]. In the present study, the combination with specific cytostatic drugs, namely AraC and mitoxantrone, increased efficacy of bortezomib. Interestingly the order of administration was crucial for the synergistic effect of the

combination. Thus preincubation with AraC followed by bortezomib revealed highest efficacy whereas the same sequence resulted in an antagonistic effect when mitoxantrone was followed by bortezomib. AraC is effective in mono- and combination therapy for MCL [44]. The synergism of AraC and bortezomib could be explained by the fact that the proteasome inhibition in AraC pretreated cells enhances the number of proapoptotic molecules and favors apoptotic pathways. In addition Sun et al. showed that during apoptosis, caspase activation results in the cleavage of three specific subunits of the 19S regulatory complex of the proteasome which inhibits the proteasomal degradation of ubiquitin-dependent and -independent cellular substrates, including proapoptotic molecules [45]. If cells are pretreated with bortezomib, induction of apoptosis and repression of the proteasome preceeds AraC incubation and incorporation of nucleoside analogs into the DNA will be slowed down. After prior bortezomib treatment, cells will be arrested in G2/M phase and DNA replication takes place only to a minor degree, thereby diminishing sensitivity to AraC. In addition bortezomib induces accumulation of the antiapoptotic Mcl-1 [46], which could reduce the efficacy of AraC. Interestingly this sequence-dependent synergistic effect was seen almost exclusively in combination with AraC.

The synergism between AraC and bortezomib shown in this study was also confirmed in primary MCL cells from four MCL patients with co-incubation of both drugs inducing synergistic apoptosis in comparison to single administration [47]. This result led to the first pilot study of this combination which has shown a high efficacy in patients with relapsed MCL [48]. Objective responses were observed in four (50%) of eight patients, including two complete remissions [48], forming the rational for a prospective randomized trial, which has recently been initiated.

On the other hand, MCL cell lines demonstrated significant antagonism if sequentially exposed to mitoxantrone, a type II topoisomerase inhibitor, followed by bortezomib thereafter while visa versa mainly additivism was reached. This is in concordance with reports that proteasomal inhibition stabilizes topoisomerase IIalpha protein and reverses resistance to the topoisomerase II poison ethonafide [49].

This sequence-dependent synergistic effect was not seen in combination with the other nucleoside analogs, fludarabine, and gemcitabine. One explanation could be their high efficiency when used for single agent treatment.

Altogether the data of the present study support the conclusion made previously by Ma and Hendershot that at least in cultured cells, activation of the unfolded protein response triggered by bortezomib can either antagonize or synergize the efficacy of chemotherapeutic drugs according to the mode of action of the drugs [50].

In summary our present study suggests a novel mechanism of bortezomib in cell cycle as well as apoptosis



regulation and specifically cautions the clinical application of bortezomib combinations dependent on the specific combination drug and sequence applied in the clinical setting.

References

- Ciechanover A (1994) The ubiquitin–proteasome proteolytic pathway. Cell 79:13–21
- Orlowski RZ, Kuhn DJ (2008) Proteasome inhibitors in cancer therapy: lessons from the first decade. Clin Cancer Res 14:1649– 1657
- Adams J (2004) The development of proteasome inhibitors as anticancer drugs. Cancer Cells 5:417–421
- 4. Montagut C, Rovira A, Albanell J (2006) The proteasome: a novel target for anticancer therapy. Clin Transl Oncol 8:313–317
- Richardson PG, Barlogie B, Berenson J et al (2003) A phase 2 study of bortezomib in relapsed, refractory myeloma. N Engl J Med 348:2609–2617
- Richardson PG, Mitsiades C, Ghobrial I, Anderson K (2006) Beyond single-agent bortezomib: combination regimens in relapsed multiple myeloma. Curr Opin Oncol 18:598–608
- Utecht KN, Kolesar J (2008) Bortezomib: a novel chemotherapeutic agent for hematologic malignancies. Am J Health Syst Pharm 65:1221–1231
- Gerecitano J, Portlock C, Moskowitz C et al (2009) Phase 2 study of weekly bortezomib in mantle cell and follicular lymphoma. Br J Haematol 146:652–655
- O'Connor OA, Moskowitz C, Portlock C et al (2009) Patients with chemotherapy-refractory mantle cell lymphoma experience high response rates and identical progression-free survivals compared with patients with relapsed disease following treatment with single agent bortezomib: results of a multicentre Phase 2 clinical trial. Br J Haematol 145:34–39
- Goy A, Bernstein SH, Kahl BS et al (2009) Bortezomib in patients with relapsed or refractory mantle cell lymphoma: updated time-toevent analyses of the multicenter phase 2 PINNACLE study. Ann Oncol 20:520–525
- 11. Suh KS, Goy A (2008) Bortezomib in mantle cell lymphoma. Future Oncol 4:149–168
- Strauss SJ, Maharaj L, Hoare S et al (2006) Bortezomib therapy in patients with relapsed or refractory lymphoma: potential correlation of in vitro sensitivity and tumor necrosis factor alpha response with clinical activity. J Clin Oncol 24:2105–2112
- Fisher RI, Bernstein SH, Kahl BS et al (2006) Multicenter phase II study of bortezomib in patients with relapsed or refractory mantle cell lymphoma. J Clin Oncol 24:4867–4874
- Jeremias I, Debatin KM (1998) TRAIL induces apoptosis and activation of NFkappaB. Eur Cytokine Netw 9:687–688
- Mitsiades N, Mitsiades CS, Richardson PG et al (2003) The proteasome inhibitor PS-341 potentiates sensitivity of multiple myeloma cells to conventional chemotherapeutic agents: therapeutic applications. Blood 101:2377–2380
- Duechler M, Linke A, Cebula B et al (2005) In vitro cytotoxic effect of proteasome inhibitor bortezomib in combination with purine nucleoside analogues on chronic lymphocytic leukaemia cells. Eur J Haematol 4:407–417
- Orlowski RZ (2005) The ubiquitin proteasome pathway from bench to bedside. Hematol Am Soc Hematol Educ Program 220– 225
- Aghajanian C, Soignet S, Dizon DS et al (2002) A phase I trial of the novel proteasome inhibitor PS341 in advanced solid tumor malignancies. Clin Cancer Res 8:2505–2511

- Orlowski RZ, Stinchcombe TE, Mitchell BS et al (2002) Phase I trial of the proteasome inhibitor PS-341 in patients with refractory hematologic malignancies. J Clin Oncol 20:4420–4427
- Pérez-Galán P, Roué G, Villamor N, Campo E, Colomer D (2007)
 The BH3-mimetic GX15-070 synergizes with bortezomib in mantle cell lymphoma by enhancing Noxa-mediated activation of Bak. Blood 109:4441–4449
- Rolland D, Camara-Clayette V, Barbarat A et al (2008) Farnesyltransferase inhibitor R115777 inhibits cell growth and induces apoptosis in mantle cell lymphoma. Cancer Chemother Pharmacol 61:855–863
- Haritunians T, Mori A, O'Kelly J, Luong QT, Giles FJ, Koeffler HP (2007) Antiproliferative activity of RAD001 (everolimus) as a single agent and combined with other agents in mantle cell lymphoma. Leukemia 21:333–339
- Heider U, von Metzler I, Kaiser M et al (2008) Synergistic interaction of the histone deacetylase inhibitor SAHA with the proteasome inhibitor bortezomib in mantle cell lymphoma. Eur J Haematol 80:133–142
- Paoluzzi L, Gonen M, Bhagat G et al (2008) The BH3-only mimetic ABT-737 synergizes the antineoplastic activity of proteasome inhibitors in lymphoid malignancies. Blood 112:2906–2916
- 25. Jones RJ, Chen Q, Voorhees PM et al (2008) Inhibition of the p53 E3 ligase HDM-2 induces apoptosis and DNA damage–independent p53 phosphorylation in mantle cell lymphoma. Clin Cancer Res 14:5416–5425
- Tabe Y, Sebasigari D, Jin L et al (2009) MDM2 antagonist nutlin-3 displays antiproliferative and proapoptotic activity in mantle cell lymphoma. Clin Cancer Res 15:933–942
- Rajkumar SV, Richardson PG, Hideshima T, Anderson KC (2005)
 Proteasome inhibition as a novel therapeutic target in human cancer. J Clin Oncol 23:630–639
- Chou TC (1991) The median-effect principle and the combination index for quantitation of synergism and antagonism. In: Chou TC, Rideout DC (eds) Synergism and antagonism in chemotherapy. Academic, San Diego, pp 61–102
- Chou TC, Talalay P (1984) Quantitative analysis of doseeffect relationships: the combined effects of multiple drugs or enzyme inhibitors. Adv Enzyme Regul 22:27–55
- Camps J, Salaverria I, Garcia MJ et al (2006) Genomic imbalances and patterns of karyotypic variability in mantle-cell lymphoma cell lines. Leuk Res 30:923–934
- Rosenwald A, Wright G, Wiestner A et al (2003) The proliferation gene expression signature is a quantitative integrator of oncogenic events that predicts survival in mantle cell lymphoma. Cancer Cells 3:185–197
- Bertoni F, Rinaldi A, Zucca E, Cavalli F (2006) Update on the molecular biology of mantle cell lymphoma. Hematol Oncol 24:22–27
- 33. Bertoni F, Ponzoni M (2007) The cellular origin of mantle cell lymphoma. Int J Biochem Cell Biol 39:1747–1753
- Schmid M, Carson D (2000) Cell cycle regulation and hematological disorders. In: Beutler E, Lichtman MA (eds) 6th edn, McGraw-Hill Professional, pp 131–140
- Muñoz-Alonso MJ, Acosta JC, Richard C, Delgado MD, Sedivy J, León J (2005) p21Cip1 and p27Kip1 Induce Distinct Cell Cycle Effects and Differentiation Programs in Myeloid Leukemia Cells. J Biol Chem 280:18120–18129
- Konicek BW, Dumstorf CA, Graff JR (2008) Targeting the eIF4F translation initiation complex for cancer therapy. Cell Cycle 15:2466–2471
- Gray NK, Wickens M (1998) Control of translation initiation in animals. Annu Rev Cell Dev Biol 14:399–458
- 38. Larsson O, Li S, Issaenko OA, Avdulov S et al (2007) Eukaryotic translation initiation factor 4E induced progression of primary human mammary epithelial cells along the cancer pathway is



- associated with targeted translational deregulation of oncogenic drivers and inhibitors. Cancer Res 67:6814-6824
- Baiz D, Pozzato G, Dapas B et al (2009) Bortezomib arrests the proliferation of hepatocellular carcinoma cells HepG2 and JHH6 by differentially affecting E2F1, p21 and p27 levels. Biochimie 91:373–382
- Li Y, Dowbenko D, Lasky LA (2002) AKT/PKB phosphorylation of p21Cip/WAF1 enhances protein stability of p21Cip/WAF1 and promotes cell survival. J Biol Chem 277:11352–11361
- Ackler S, Ahmad S, Tobias C, Johnson MD, Glazer RI (2002)
 Delayed mammary gland involution in MMTV-AKT1 transgenic mice. Oncogene 21:198–206
- Li X, Liu J, Gao T (2009) beta-TrCP-mediated ubiquitination and degradation of PHLPP1 are negatively regulated by Akt. Mol Cell Biol 29:6192–6205
- 43. Ma MH, Yang HH, Parker K et al (2003) The proteasome inhibitor PS-341 markedly enhances sensitivity of multiple myeloma tumor cells to chemotherapeutic agents. Clin Cancer Res 9:1136–1144
- Dreyling, MH and Hiddemann W (2009) Current treatment standards and emerging strategies in mantle cell lymphoma. Hematology, ASH Education Program Book: 542–551

- Sun XM, Butterworth M, MacFarlane M, Dubiel W, Ciechanover A, Cohen GM (2004) Caspase activation inhibits proteasome function during apoptosis. Mol Cell 14:81–93
- 46. Pérez-Galán P, Roué G, Villamor N, Montserrat E, Campo E, Colomer D (2006) The proteasome inhibitor bortezomib induces apoptosis in mantle-cell lymphoma through generation of ROS and Noxa activation independent of p53 status. Blood 107:257–264
- Weigert O, Pastore A, Rieken M, Lang N, Hiddemann W, Dreyling M (2007) Sequence-dependent synergy of the proteasome inhibitor bortezomib and cytarabine in mantle cell lymphoma. Leukemia 21:524–528
- 48. Weigert O, Weidmann E, Mueck R et al (2009) A novel regimen combining high dose cytarabine and bortezomib has activity in multiply relapsed and refractory mantle cell lymphoma—long-term results of a multicenter observation study. Leuk Lymphoma 50:716–722
- Congdon LM, Pourpak A, Escalante AM, Dorr RT, Landowski TH (2008) Proteasomal inhibition stabilizes topoisomerase IIalpha protein and reverses resistance to the topoisomerase II poison ethonafide (AMP-53, 6-ethoxyazonafide). Biochem Pharmacol 75(4):883–890
- Ma Y, Hendershot LM (2004) The role of the unfolded protein response in tumour development: friend or foe? Nat Rev Cancer 4 (12):966–977

